www.ptcer.pl/mccm

MATERIAŁY CERAMICZNE /CERAMIC MATERIALS/, 65, 3, (2013), 258-266

Mechanical properties and low temperature degradation resistance of 2.5Y-TZP – alumina composites

Frank Kern*, Rainer Gadow

University of Stuttgart, IFKB, D-70569 Stuttgart, Allmandring 7B
*e-mail: frank.kern@ifkb.uni-stuttgart.de

Abstract

Yttria stabilized zirconia polycrystals (Y-TZP) become increasingly important in the field of biomedical and engineering components. The commercially available standard material 3Y-TZP made from coprecipitated powders has very high strength but limited fracture toughness, resistance to subcritical crack growth and low temperature degradation resistance. In this study a 2.5Y-TZP powder was produced by coating of monoclinic zirconia with yttria via the nitrate route. Y-TZP-alumina composites with compositions ranging from 0-27.5 vol.% were produced by mixing and milling and subsequent hot-pressing at 1400 °C for 2 h. The mechanical properties and ageing resistance of the materials was tested. All materials showed attractive mechanical properties with bending strength of 1000-1250 MPa, fracture resistance declined with increasing alumina content while resistance to subcritical crack growth K_{I0} was maintained at a high level of 5–5.7 MPa·√m. Alumina addition had a non-linear grain growth inhibition effect. Ageing test showed that while the pure 2.5-TZP was inherently instable a small addition of alumina increased the low temperature ageing resistance considerably. Evaluation of ageing kinetics according to the Mehl-Avrami-Johnson model showed that the TZP-alumina composites did not follow a nucleation and growth mechanism but that the transformation front rather proceeds into the bulk by a zero-order kinetics.

Keywords: Degradation resistance, Mechanical properties, Y-TZP, Alumina, Composite

WŁAŚCIWOSCI MECHANICZNE I ODPORNOŚĆ NA NISKOTEMPERATUROWĄ DEGRADACJĘ KOMPOZYTÓW 2.5Y-TZP – TLENEK GLINU

Polikryształy dwutlenku cyrkonu stabilizowanego tlenkiem itru (Y-TZP) stają się coraz ważniejsze w obszarze komponentów biomedycznych i inżynierskich. Komercyjnie dostępny, standardowy materiał 3Y-TZP wytworzony z proszków współstrąconych ma bardzo wysoką wytrzymałość ale ograniczoną odporność na pękanie, odporność na podkrytyczny wzrost pęknięcia i odporność na niskotemperaturową degradację. W niniejszej pracy, proszek 2.5Y-TZP wytworzono drogą pokrywania jednoskośnego tlenku cyrkonu tlenkiem itru metodą azotanową. Kompozyty Y-TZP-tlenek glinu o składach mieszczących się w przedziale (0-27,5)% obj. wytworzono drogą mieszania i mielenia z następczym prasowaniem na gorąco w 1400 °C przez 2 h. Zbadano właściwości mechaniczne i odporność na starzenie otrzymanych materiałów. Wszystkie materiały pokazały atrakcyjne właściwości mechaniczne: wytrzymałość na zginanie 1000-1250 MPa, odporność na pękanie zmniejszyła się wraz ze wzrostem zawartości tlenku glinu, podczas gdy odporność na podkrytyczny wzrost pęknięcia K_{I0} utrzymywała się na poziomie 5–5,7 MPa·√m. Dodatek tlenku glinu wywołał nieliniowy efekt zahamowania rozrostu ziaren. Test starzenia wykazał, że wtedy gdy czysty 2.5-TZP był zasadniczo niestabilny to mały dodatek tlenku glinu zwiększał znacząco niskotemperaturową odporność na starzenie. Wyznaczenie kinetyki starzenie zgodnie z modelem Mehl-Avrami-Johnsona wykazało, że kompozyty TZP-tlenek glinu nie podlegają mechanizmowi zarodkowania i wzrostu zarodków, ale raczej front przemiany podąża w materiał zgodnie z kinetyką reakcji rzędu zerowego.

Słowa kluczowe: odporność na degradację, właściwości mechaniczne, Y-TZP, Al_2O_3, kompozyt

1. Introduction

The high strength and toughness of zirconia structural ceramics is determined by the effect of transformation toughening, a stress induced phase transformation from the metastable tetragonal to the stable monoclinic phase which is associated with volume expansion and shear [1]. For applications requiring high strength such as dental implants or engineering components, commonly Y-TZP stabilized with 2.5-3.5 mol.% of yttria is used which reaches strength of > 1000 MPa and fracture resistance values of 4-6 MPa·√m depending on stabilizer content and sintering conditions/ grain size [2]. Unfortunately the toughest materials suffer from a drawback resulting from poor low temperature degradation resistance. In contact with moisture a spontaneous non stress induced transformation to monoclinic takes place which limits the exposition time and temperature in moist environments [3]. Especially in case of biomedical implants this effects become important, ageing induced failure of Y-TZP femoral heads have led an almost complete elimination from this application and replacement by ZTA materials [4]. Y-TZP has become a standard material for dental crowns

and bridges, the trend for metal free solutions in dental implants has attracted increasing interest in ceramic solutions for replacement of the implant itself which nowadays is made predominantly of titanium alloys [5].

Recent studies have shown that the set of requirements to mechanical properties and ageing resistance of ceramic materials for implants are complex and do in some cases exceed the definitions of EN ISO 6872.

Implants are repeatedly loaded components which makes resistance to subcritical crack growth more important than the strength as such. Effective biting force at second molar may reach 600 MPa [6]. In fact a standard Y-TZP just fulfilling the standard (σ = 800 MPa, K_{IC} = 5 MPa·√m) reaches its limits as K_{I0} is only with 2.5-3 MPa·√m [6]. Under subcritical conditions the component can only be repeatedly loaded to $\sigma_{SC} = \sigma \cdot (K_{I0}/K_{IC})$ = 400-480 MPa. Threshold toughness K_{I0} of materials for dental implants should thus be as close as possible to K_{IC}, strength should be high and considering a possible damaging of the component during manufacturing, implantation or use, the fracture resistance K_{IC} should also be as high as possible. Ageing resistance is also an important issue, at a projected lifetime of 10-30 years for an implant the material should stand 3-10 hours of a standard autoclave test (134 °C) without severe degradation. Ageing is not only an issue of surface degradation or a deterioration of mechanical properties. Transformation induced residual stress in the components adds to the applied stress and may lead to premature failure. New developments in implant design including coatings or roughened surfaces to improve the ingrowth and fixation of the implant in the jaw may even increase the demands concerning LTD as increased surface area or mechanical or chemical impact may reduce the ageing resistance of the component surface compared to the properties of the bulk material.

In recent years several concepts have been elaborated to overcome these problems. Binner has shown that 3Y-TZP of nanoscale small grain size has extremely high ageing resistance. However these materials also become almost untransformable by stress and thus have a limited fracture resistance [8]. Shifting from Y-TZP to tougher and much more ageing resistant Ce-TZP based composites may also be a feasible way to solve the problem. Recently a Ce-TZP/spinel composite was reported having a strength of > 900 MPa and a toughness of 15 MPa and a threshold toughness of 8 MPa·√m. [9]

Staying with Y-TZP but changing from coprecipitated to yttria coated powders leads to a considerable gain in toughness and little effect on strength [10]. During sintering the stabilizer diffuses into the grains producing a stable shell and an extremely transformable core [11]. It was even claimed that these materials show no ageing at all [12]. According to own results this interpretation is too optimistic, however higher aging resistance can be achieved at lower stabilizer contents and maintaining higher fracture toughness [13]. Alumina addition to TZP even in small amounts is known to improve ageing resistance as the alumina is incorporated into the first atomic layers of the zirconia grain boundaries leading to higher stability of the tetragonal phase [14]. Larger fractions of alumina are contained in alumina toughened zirconia with higher strength and improved ageing resistance compared to Y-TZP [15,16]. It was shown in a previous paper that large fractions of alumina significantly reduce fracture toughness of 2.5Y-TZP [17]. In the present study the role of the alumina content on mechanical properties and ageing resistance of Y-TZP derived from yttria coated powder is studied systematically. The stabilizer content was set to 2.5 mol.%, a composition very close to the t/t+c phase boundary having a high inherent instability in undoped state. Hot pressing was chosen due to the limited amounts of starting powder available.

2. Experimental

The powder preparation process basically followed a process previously described by Yuan [18], the procedure was slightly modified to obtain less hard agglomerated powders. Starting powders for the synthesis of 2.5Y-TZP were TZ-0 (Tosoh, Japan) an agglomerated nanopowder with a specific surface area of 14-19 m²/g and a primary crystallite size of 25 nm (manufacturer's specification) and yttria (Aldrich, USA) with a purity of 99.9%. Two batches of 400 g 2.5Y-TZP were produced each consisting of 17.5 g yttria and 372.5 g zirconia. The yttria was dissolved in boiling half concentrated nitric acid and added to the zirconia previously dispersed in 600 ml 2-propanol. 1 kg of Y-TZP milling balls (d = 5 mm) were added and the mixture was milled overnight to de--agglomerate the zirconia and homogeneously disperse the nitrate. Then the 2-propanol was evaporated at 130 °C and the dried intermediate was heated to 350 °C for 3 h to convert the yttrium nitrate to oxide. Then the powder was crushed and passed through a 125 µm screen. The screened powder was then calcined at 800 °C for 1 h in air. Finally the resulting 2.5Y-TZP was blended with alumina to obtain mixtures with 0, 0.5, 2, 5, 10 and 27.5 vol.% of alumina. The blends were subsequently milled for 4 h in 2-propanol with Y-TZP milling balls of 1 mm in diameter. The ready to use hot pressing powders were then obtained from the dried and screened suspensions. Samples are named 2.5Y-XAl meaning 2.5Y--TZP with X vol.% alumina.

Hot pressing (KCE, Germany) was carried out in vacuum in a boron nitride clad graphite mould of 45 mm diameter. Heating to final temperature of 1400 °C was carried out at 50 K/min under 3 kN pre-load. When the final temperature was reached the load was increased to 40 MPa and maintained during the 2 h dwell. Two samples of 2.5 mm thickness separated by a graphite disk were pressed during one cycle, samples were cooled in the press with the heater shut off.

The resulting disks were then lapped with 15 µm diamond suspension, polished with 15 µm, 6 µm and 1 µm suspension for 30 min each to obtain a mirror like finish (Struers, Rotopol, Denmark). The disks were then cut into 7 bars of 4 mm × 2 mm diameter (Struers, Accutom, Denmark). Remaining pieces were kept for hardness testing and ageing tests. The bars were then lapped on the sides with 15 µm diamond suspension to eliminate the cutting grooves, edges were carefully bevelled.

Mechanical testing included measurement of Vickers hardness HV0.1 (Fischer, Germany) and HV10 (Bareiss, Germany), the indentation modulus E_{IND} was calculated from the loading/unloading curve of the microhardness measurement. The bending strength was measured in a 4-pt setup with 20 mm outer and 10 mm inner span at a crosshead

speed of 0.5 mm/min on 10 samples (Zwick, Germany). The fracture resistance was determined in the same test setup by ISB (indentation strength in bending) on three samples [19]. Bars were pre-notched with a HV10 indent parallel and perpendicular to the sides on middle of the tensile side, samples were tested immediately after indentation, the crosshead speed was 2.5 mm/min.

The resistance to subcritical crack growth was determined by stable indentation crack growth in bending (SIGB) according to a procedure described by Dransmann and Benzaid [20,7]. Two bending bars of each composition were indented in the middle of the tensile side in the area between the inner span of the testing equipment, four HV10 indents were placed in line at a distance of 2 mm. The samples were then left to rest for two weeks so that the cracks could grow sub-critically to a stable extension. The samples were then successively loaded at a crosshead speed of 5 mm/min with increasing bending stress. The starting stress was set to 75 MPa, the stress then was increased in 25 MPa increments until failure. The length of the cracks normal to the sides was measured optically after each loading step. The indentation procedure after release of the load causes a crack closing residual stress intensity in the samples. The crack starts to grow when the applied stress intensity $K_{app} = \psi \cdot \sigma \cdot \sqrt{c}$ overcomes this residual stress intensity $K_{res} = \chi \cdot P \cdot c^{-1.5}$. Here c = crack length, σ = bending stress, P = indentation load and ψ = 1.27 shape factor, χ = residual stress coefficient. Plotting $\psi \cdot \sigma \cdot \sqrt{c}$ versus $P \cdot c^{-1.5}$ leads to a graph with two characteristic points, the value $K_{app,0}$ indicates the stress intensity from which the crack starts to grow, the intercept of the resulting straight line with the ordinate indicates the value K_{IC}, the critical stress intensity at infinite crack length. The slope of the straight line is χ. The threshold stress intensity marking the resistance to subcritical crack growth is given by $K_{I0} = K_{IC} - K_{app,0}$. $K_{app,0}$ is the R-curve dependent part of the stress intensity.

The phase composition of the materials was determined by XRD. Monoclinic contents of polished surfaces $V_{m,pol}$ and fracture faces $V_{m,FF}$ were investigated (Bruker, Germany, CuKα radiation, graphite monochromator). The intensity of the monoclinic (111) and (-111) reflexes as well as the tetragonal (101) reflex were measured in the 27-33° 2θ-range. The difference between both values is the transformed fraction $V_f = V_{m,FF} - V_{m,pol.}$ The quantitative analysis was carried out using the calibration curve of Toraya [21]. The same procedure was used to measure the phase compositions of aged samples. The transformation depth h in the fractured faces can be determined from these data using the formalism described by Kosmac [22]. According to McMeeking [23] the transformation toughness increment $K_{IC}{}^{T}$ is, eq. 1:

$$\Delta K_{IC}{}^{T} = \frac{X}{1-\nu} \cdot V_f \cdot E \cdot \varepsilon_T \cdot \sqrt{h} \qquad (1)$$

Here E is the elastic modulus, ν the Poisson' ratio, and ε_T the transformation related volume expansion (0.05), X is a factor specific for the transformation behaviour (X = 0.22 for pure dilatation), for Y-TZP X = 0.27 [2]. A tentative determination of the crack tip toughness of the TZP was carried out by plotting K_{IC} versus the product of the transformed fraction V_f and transformation zone depth h. The resulting intercept is the crack tip toughness K_{tip} describing the "intrinsic" fracture resistance before the crack tip (not to be confused with K_{I0} !).

The accelerated ageing tests to determine the low temperature degradation resistance in saturated water vapour were carried out in an autoclave at 134 °C at exposition times of 1 h, 3 h, 10 h 30 h and 100 h dwell. Phase compositions were measured by XRD. Changes in surface roughness with ageing time were investigated by tactile roughness measurement (Mahr, Perthometer, Germany).

The microstructures of the polished and etched samples (1200 °C, 10 min, air) were studied by SEM (Zeiss Gemini, Germany) in SE mode using in-lens technology at low acceleration voltage of 3kV. The grain sizes were determined by linear intercept method following the calculation scheme of Mendelsson [24].

Images of the aged surfaces were made by optical microscopy using differential interference contrast DIC (Zeiss, Germany). The density of the materials was measured by buoyancy method.

3. Results

3.1. Mechanical properties

Hardness HV10 and indentation modulus E_{IND} of the TZP-alumina composites is shown in Fig. 1. Both values, hardness and stiffness, increase with increasing alumina content as can be expected from the rule of mixture. It should be taken into account that the indentation modulus is systematically too high by ~ 10%, for pure zirconia a value of 210-230 GPa would be expected.

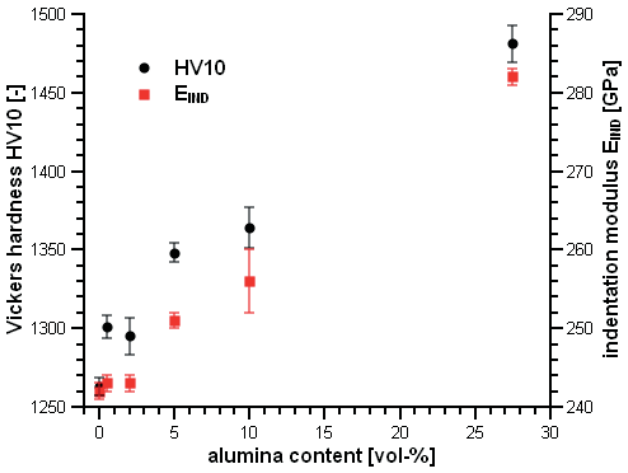

Fig. 1. Vickers hardness HV10 and indentation modulus E_{IND} of 2.5Y-TZP – alumina composites.

The 4-pt bending strength and fracture resistance according to the ISB method are presented in Fig. 2. The bending strength of the different 2.5Y-TZP-alumina composites ranges between 1000 MPa and 1250 MPa. A systematic dependency on alumina content cannot be detected. The fracture resistance K_{ISB} shows a very clear trend to decline with increasing alumina content. The highest fracture resistance of K_{ISB} = 7.4 MPa·√m is observed for the alumina free compound, whereas the alumina toughened zirconia with 27.5 vol.% alumina (20 wt.%) has the lowest toughness K_{ISB} = 6 MPa·√m.

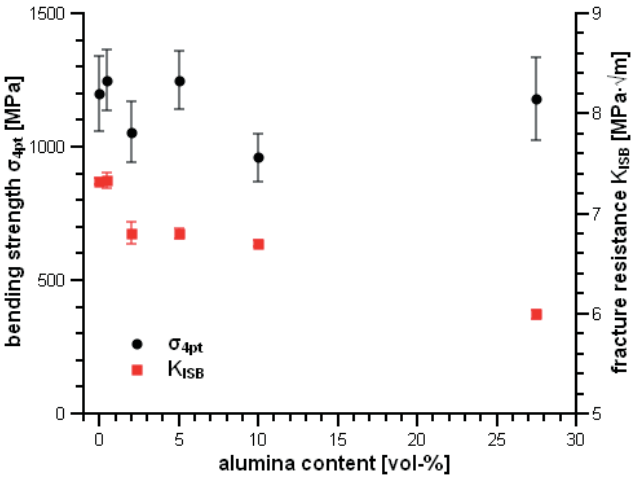

Fig. 2. Bending strength σ_{4pt} and fracture resistance K_{ISB} of 2.5Y-TZP – alumina composites.

The measurements of K_{I0}, the resistance against subcritical crack growth, of representative compositions containing 0 vol.%, 0.5 vol.%, 5 vol.% and 27.5 vol.% of alumina are shown in Fig. 3. The data points shown are the averages of four measurements each with the corresponding standard deviations determined by variations in the measured the crack length *c*. At the right side of the curves at low crack length (X-axis plots ~ $1/c^{1.5}$) the first measurement points are on a vertical line, when the applied stress intensity overcomes the stored residual stress intensity, the cracks start to grow.

In the plots the kink of the curve indicates the value $K_{app,0}$, the ordinate intercept corresponds to K_{IC}, K_{I0} can be determined from the difference of K_{IC} and $K_{app,0}$. As all samples develop relatively long cracks ($2c$ ~ 0.5 mm) the quality of the regressions is very good and reliable extrapolations can be carried out. It is however clearly visible that there is some non-linearity in the long-crack area, these measurements were not included in the linear regression to determine K_{IC}.

The results of SIGB measurements of all materials are summarized in Fig. 4. The measurements show a clear tendency. The fracture resistance K_{IC} as well as the R-curve dependent part of fracture resistance $K_{app,0}$ decline with increasing alumina content. The combination of both, K_{I0} the resistance to subcritical crack growth, stays in the range between 5-5.7 MPa·√m. The local minimum at low alumina contents (0.5-2 vol.%) is statistically not very significant considering the addition of standard deviations from two measurements in calculation of K_{I0}. The extrapolated fracture resistance K_{IC} shows an identical tendency as K_{ISB}. The extrapolated fracture resistances are systematically ~ 0.5 MPa·√m higher than the values of K_{ISB}.

3.2. Phase composition

Measurements of phase composition of the polished surface representing the bulk of the material and fracture phases (Fig. 5) revealed that alumina addition leads to a significant change in transformability.

The monoclinic contents in the bulk decline exponentially with increasing alumina addition, the pure TZP has 7 vol.% of monoclinic, in composites with ≥ 5 vol.% alumina no monoclinic can be detected. This reflects the stabilizing effect of alumina which at a certain point seems to run into saturation. The monoclinic content in the fracture faces however does not follow this tendency. An increase from 0% to 0.5% alumi-

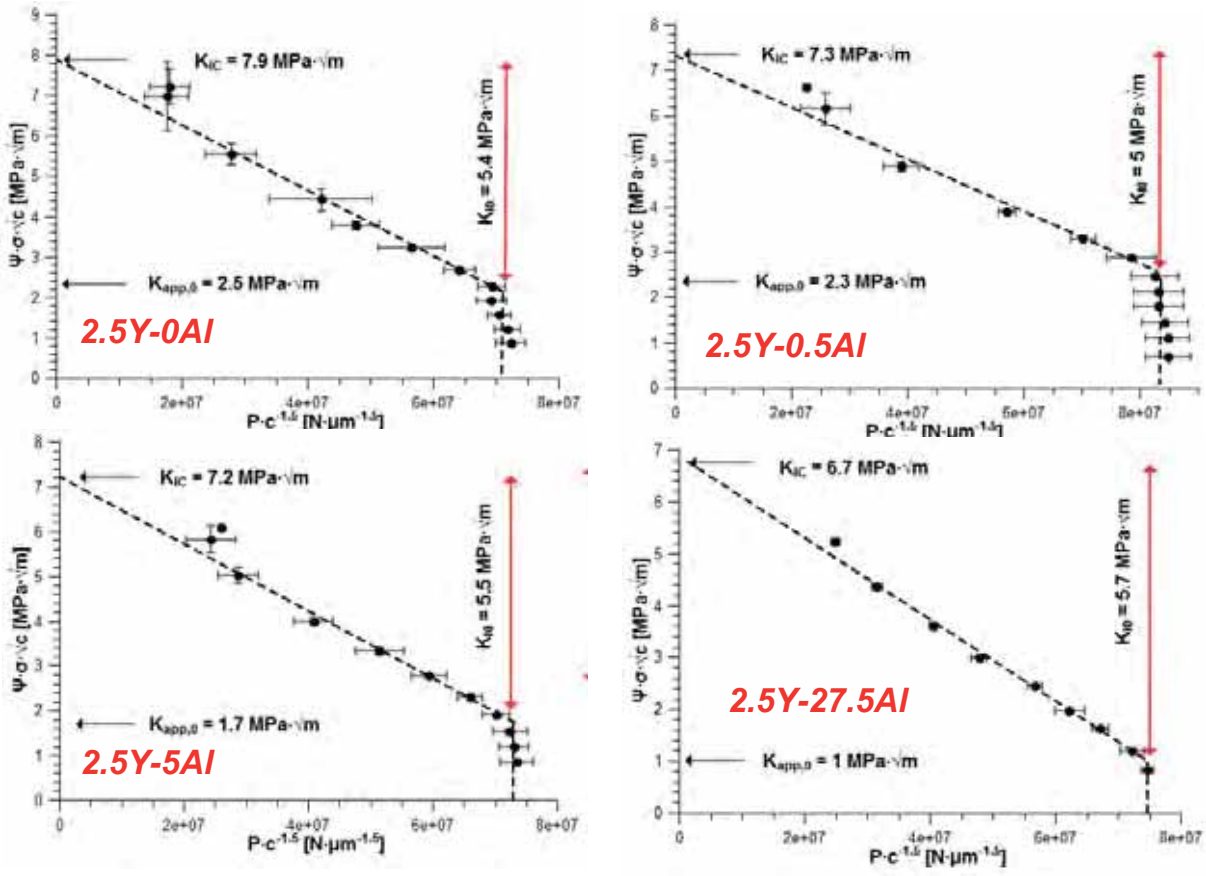

Fig. 3. Plots of SIGB measurements of four characteristic Y-TZP-alumina compositions.

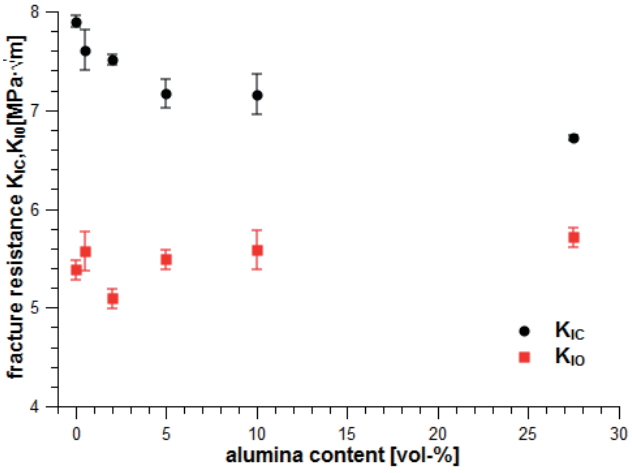

Fig. 4. Extrapolated fracture resistance K_{IC} and resistance to sub-critical crack growth K_{I0} 2.5Y-TZP – alumina composites determined by SIGB.

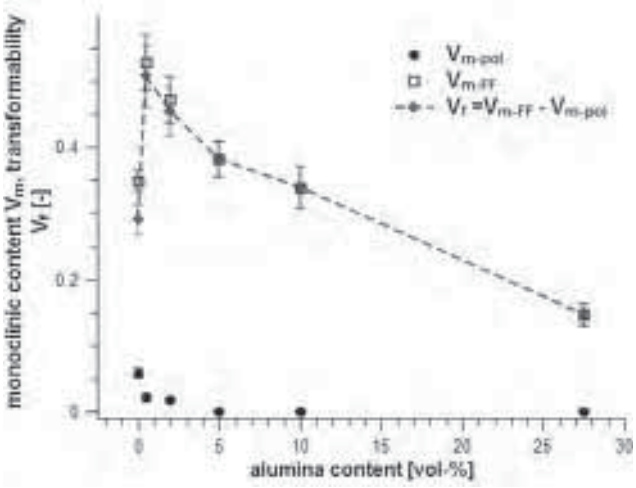

Fig. 5. Monoclinic content in polished surfaces and fracture faces and resulting transformability of 2.5Y-TZP – alumina composites determined by XRD.

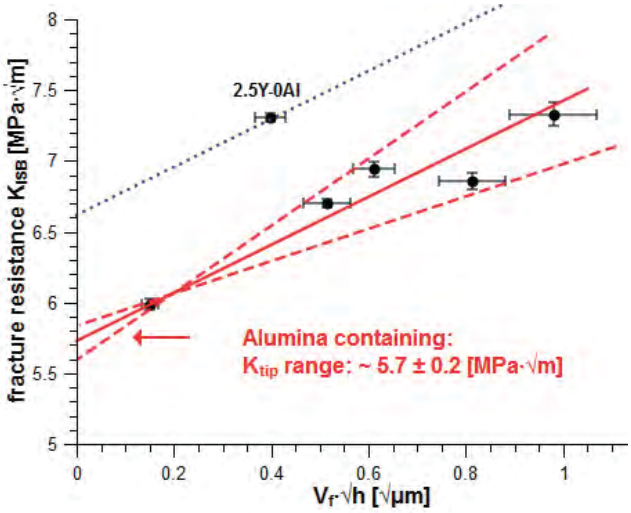

Fig. 6. Fracture resistance K_{ISB} versus the product of V_f·√h, tentative extrapolation to crack tip toughness K_{tip}.

na increases the monoclinic fraction drastically from 35% to 53%. Then with rising alumina contents monoclinic contents decrease. The transformability V_f increases from 30% to 50% with addition of 0.5 vol.% alumina and falls almost linearly to 17% in case of the material containing 27.5 vol% alumina.

The corresponding values of transformation zone depth *h* and transformation toughness increment K_{IC}^T follow the trend of transformability (not shown). K_{IC}^T rises from 1.7 MPa·√m to 4.4 MPa·√m from 0% to 0.5% alumina, then declines to 0.6 MPa·√m for the highest alumina content. Transformation zone *h* rises from 1.8 µm to 3.7 µm from 0% to 0.5% alumina, then declines to 1 µm for the highest alumina content. The zone sizes *h* are well in the range reliably measurable by XRD.

Evidently the trends in transformability and fracture resistance are similar for the alumina containing materials. In case of the pure TZP the fracture resistance seems too high with respect to the transformed fraction. This relation is visualized in Fig. 6 plotting the fracture resistance K_{ISB} versus the product of V_f·√h.

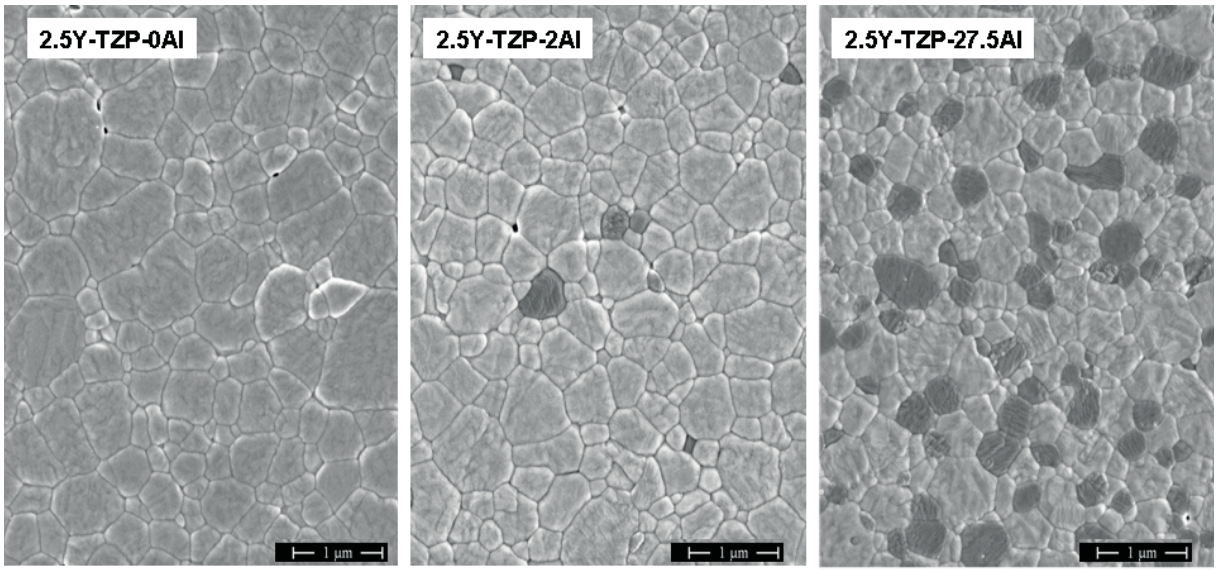

Fig. 7. SEM images of polished and thermally etched surfaces of 2.5-TZP alumina composites.

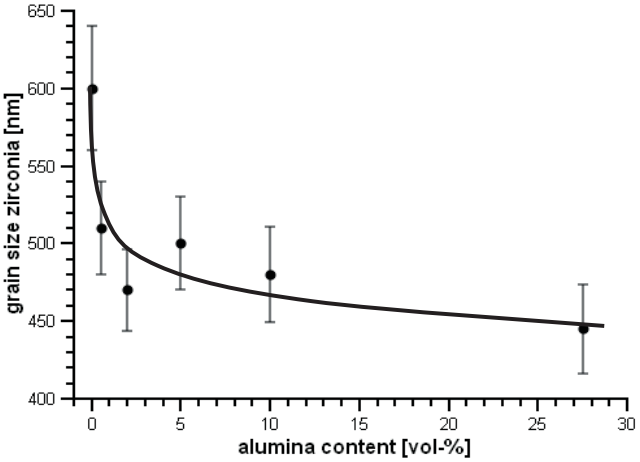

Fig. 8. Grain sizes of zirconia grains in 2.5Y-TZP-alumina composites vs. alumina content determined by line intercept method from SEM images.

Assuming a predominantly dilatoric transformation behaviour and a factor of $X = 0.27$ (see eq. 1), the regression line to zero transformability ($V_f \cdot \sqrt{h} = 0$) through the data of alumina containing materials intercepts at K_{tip} = 5.7 ± 0.2 MPa·√m. The total fracture resistance is determined as the sum of the intrinsic toughness and contribution from all reinforcing mechanisms ($K_{IC} = K_{tip} + \sum \Delta K_{IC}^{R}$). For the behaviour of the pure TZP there are three possible explanations. We may either assume that in case of the pure TZP there are reinforcing mechanisms active besides transformation toughening, the material may have a different crack tip toughness or that the character of the transformation is different with a higher contribution of shear (X → 0.48 in eq.1).

3.3. Microstructure

Fig. 7 shows SEM images of the thermally etched surfaces of materials containing 0 vol.%, 2 vol.% and 27.5 vol.% alumina. The grain refinement by addition alumina is clearly visible, the distribution of the alumina in the composite containing 27.5% is very homogeneous. Alumina grains, due to the moderate sintering temperature, have not significantly grown compared with the average grain size of the starting powder (300 nm). While the density measurements showed that the materials are fully dense, some porosity in the SEM images of samples of low alumina content is visible. This apparent porosity is probably an artefact of the thermal etching process in air. After pressing samples are oxygen deficient having colours shifting from black (low alumina content) to dark grey (high alumina content). During the etching process carried out at rapid heating in order not to over-etch the samples for SEM, take-up of oxygen leads to a whitening and due to changes in the elementary cell size locally to residual stress induced formation of pores or even small cracks.

Fig. 8 summarizes the results of the zirconia grain size measurements by line intercept method. Again the most significant change happens between 0% and 0.5% alumina. Addition of the dopant reduces the average grain size from 600 nm to 510 nm. Further addition in excess to 0.5% is less efficient. 2.5Y-27.5Al has a grain size of 450 nm. As larger

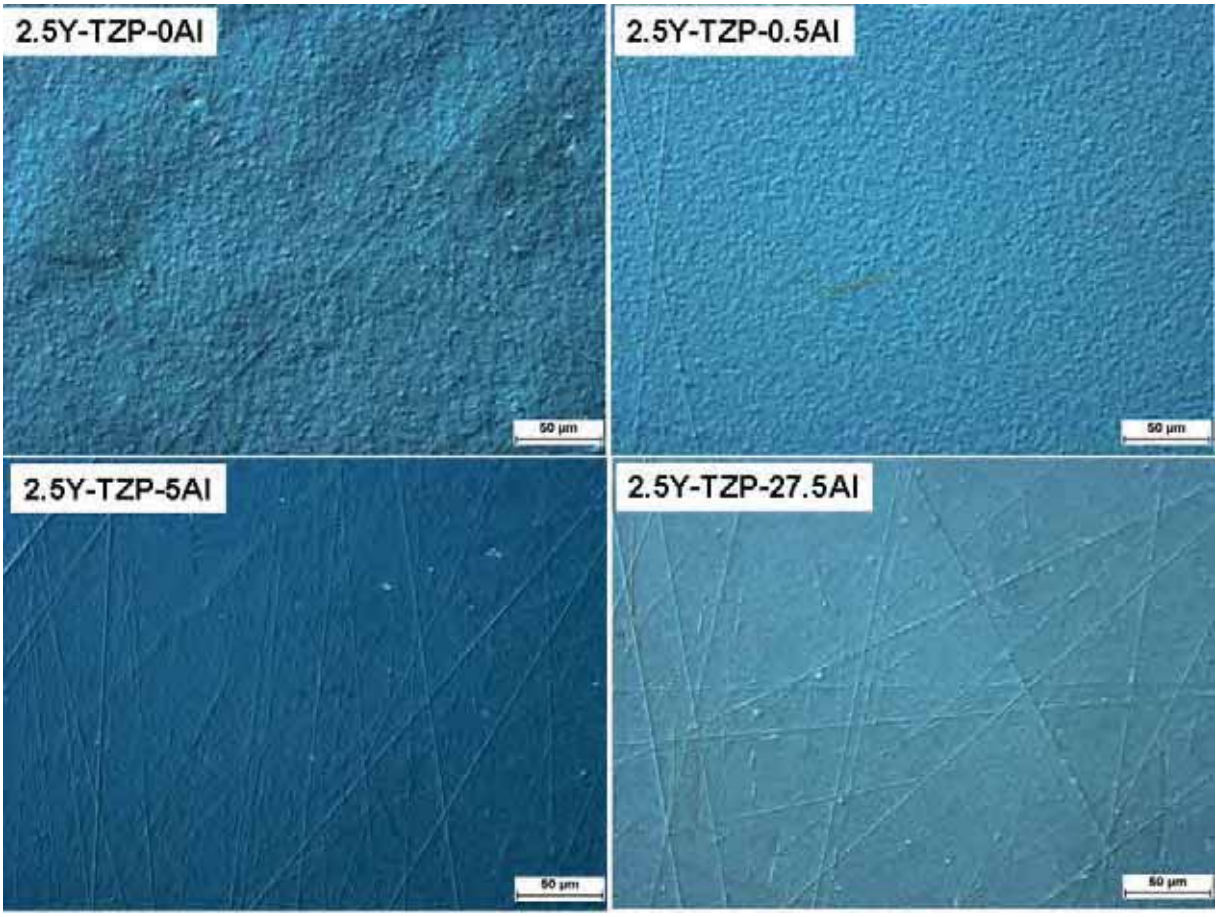

Fig. 9. Light microscope images of polished and surfaces of 2.5Y-TZP-alumina composites exposed to water vapour in an autoclave at 134 °C for 10 hours (topography visualized by differential interference contrast).

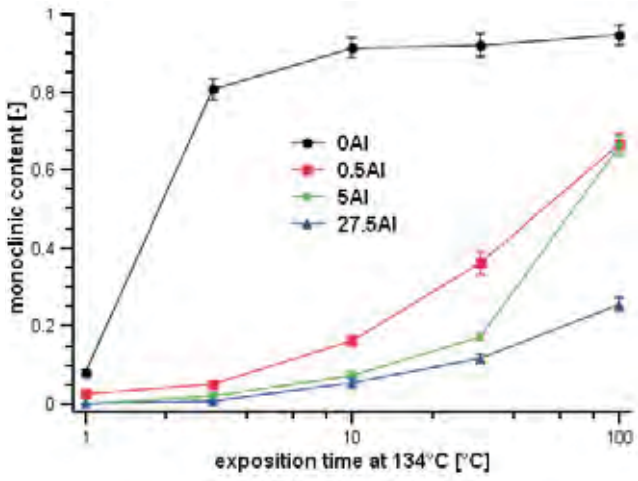

Fig. 10. monoclinic contents in surfaces of aged TZP-alumina composites vs. exposition time in autoclave.

zirconia grains are more transformable the microstructural features are in good accord with the toughness measurements and phase analysis. This is however only true for the alumina containing materials, again the undoped TZP does not fit into this scheme.

3.4. Low temperature degradation resistance

Fig. 9 shows light microscope images of surfaces of materials aged 10 hours in water vapour in an autoclave. This exposition time corresponds to the projected lifetime of an implant which is approximately 30-40 years *in vivo*. The images show clearly that the alumina-free TZP is strongly transformed. Not only the roughness is very high (R_z = 0.35 µm), also significant waviness can be clearly detected (W_t = 0.35 µm). The material containing 0.5 vol.% alumina shows some ageing effects, roughness and waviness are significantly lower (R_z = W_t = 0.22 µm). Materials of higher alumina content seem virtually unaffected by the ageing treatment, only along some preparation derived grooves nucleation of monoclinic can be detected. Roughness (R_z < 0.13 µm) and waviness (W_t < 0.1 µm) are significantly lower for materials containing 5% of alumina or more. Extended ageing experiments for 100 h (images not shown) affects all samples, in case of the pure TZP the piled up residual stress by phase transformation results in a further increase of waviness (W_t < 1 µm) and the destruction of the sample by severe spallation of the transformed layer. In case of the alumina containing materials the ageing proceeds in a more controlled way, roughness continuously increases, the 2.5Y-27.5Al is least affected. Concerning the tactile roughness and waviness measurements it should be noted that a certain threshold in the unaged samples exists ($R_{z,0}$ = 0.1-0.12 µm, $W_{t,0}$ = 0.1 µm). The monoclinic contents with in some selected composites are shown in Fig. 10.

Evidently the monoclinic content in the pure TZP reaches a very high level of 80% after a short aging time of 3 h. According to Kosmac this corresponds to a transformation depth of ~ 10 µm or more [22]. The XRD measurements of materials at higher exposition times cannot give any quantitative information about the progress of the phase transformation into the bulk of the material. Alumina containing composites show a smooth increase of monoclinic content.

In the MAJ-equation (eq.2) the monoclinic content V_m is dependent on time, and two coefficients, *b* the rate constant and *n* the Avrami-exponent [3].

$$V_m = 1 - \exp^{(b \cdot t)^n} \qquad (2)$$

In a linearized plot of ln(ln(1-V_m)) versus ln(t/*dim*(t)) the slope of the line is the Avrami exponent *n*, the axis intercept is ln(*b*) the logarithm of the rate constant (Fig. 11).

Evidently the axis intercepts decrease with increasing alumina content reflecting the observed higher aging resistance induced by alumina addition. Except for the line for 2.5Y-0Al (which is completely transformed at t < 3 h) the slopes *n* are very close to 1.

2.5Y-27.5Al shows some non-linearity of slope, Avrami coefficients are higher (*n* = 1.2) for short exposition times and lower (*n* = 0.8) at prolonged ageing. Contrary to literature data which suggest that the aging proceeds as a nucleation and growth mechanism with *n* = 3-4, the ageing process seems to follow a simple first order kinetics (V_m = 1- exp$^{(b \cdot t)}$). This process is however superposed by the absorption of the X-rays in the material which should follow Lambert-Beer's law (eq. 3).

$$-\ln\left(\frac{I}{I_0}\right) = \varepsilon^* \cdot c \cdot d \qquad (3)$$

Here ε* corresponds to the X-ray absorption coefficient, *d* to the layer thickness (~ 10 µm) and I_0 the initial intensity and *I* the intensity at a depth *d*, *c* corresponds to the concentration V_m. Considering the effect of X-ray absorption a zero order kinetics is obtained, this means that the monoclinic layer proceeds into the bulk at constant velocity. This result is in good accord to recent results of Keuper who studied the progress of the transformation on sections made by focused ion beam and compared the results of XRD data [25].

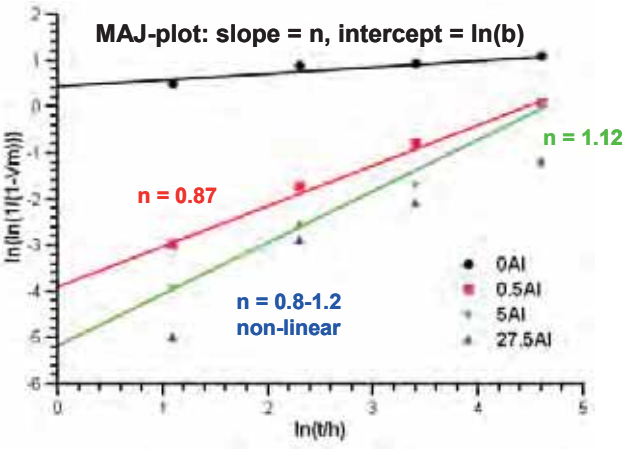

Fig. 11. MAJ plot of the ageing behaviour of different TZP-alumina composites.

4. Discussion

The results have shown that among all materials tested pure 2.5Y-TZP has good mechanical properties, high strength, highest fracture resistance and high threshold toughness. Phase analysis in combination with fracture resistance measurements has revealed that the alumina free material is fundamentally different, according to the common theory [26] the large grain size should guarantee a high trans-

formability, however this is not the case. The transformability of the material is limited, the high fracture resistance is therefore probably not caused by high transformation toughness but most probably by a much higher crack tip toughness (K_{tip} ~ 6.5 MPa·√m) than in the alumina containing materials. The favourable mechanical properties may, however, only be exploited under absolutely dry conditions. The material is not suitable for biomedical applications as the autoclave test has shown that it completely deteriorates within short exposition times.

The alumina containing materials show properties steadily changing with alumina content. While hardness and stiffness basically follow the rule of mixture the strength seems independent on alumina concentration. Fracture resistance and transformability and as a result transformation depth and transformation toughness increments decline with increasing alumina content. Threshold toughness stays at a high level of 5-5.7 MPa·√m. The crack tip toughness of the materials can be estimated at ~ 5.7 MPa·√m. Alumina doped Y-TZP materials made from yttria coated powders are thus very interesting materials for different kinds of applications. Composites containing a large fraction of alumina like the 2.5Y-27.5Al have a threshold fracture resistance close the absolute fracture resistance. With a strength of 1200 MPa and a ratio (K_{I0}/K_{IC} = 0.85) it can be calculated that they can be safely applied under cyclic loads of up to σ_{SC} ~ 1000 MPa without risking failure by subcritical crack growth. Composites with lower amounts of alumina such as 2.5Y-0.5Al (σ = 1250 MPa, K_{I0}/K_{IC} = 0.73) may be operated up to 900 MPa, here the higher R-curve related toughness will provide an additional safety buffer to avoid single catastrophic events.

The low temperature degradation resistance of the TZP-alumina composites is very high with regard to the low stabilizer content of the matrix material and increases considerably with rising alumina content. Compared to data measured by Chevalier for 3Y-TZP the rate constants of the alumina doped materials are lower by a factor of 2-3 and the Avrami exponents are close to unity meaning that the ageing proceeds much slower with increasing exposition times. This corresponds to the observations of a very smooth increase of monoclinic content in contrary to the very abrupt transformation of 3Y-TZP during relatively short time increments [3]. However a complete insensitivity to aging as claimed by Picconi cannot be observed even in case of the highest alumina content [12]. The study of the ageing kinetics shows that the transformation front proceeds into the bulk of the material with constant speed. Alumina addition can retard but not prevent ageing. Results also seem to indicate that the relation between martensitic transformation induced by stress and transformation induced by ageing is not strictly coupled but can be influenced by stabilizing dopants such as alumina.

5. Summary

2.5Y-TZP alumina composites of various alumina contents were produced from yttria coated monoclinic powders by mixing and milling and subsequent hot pressing. Mechanical properties, phase compositions and microstructures were investigated, the resistance to low temperature degradation resistance was evaluated by an accelerated ageing test.

Alumina addition even in low amounts changes the transformation toughening characteristics and ageing resistance of the 2.5Y-TZP drastically. The plain TZP shows excellent mechanical properties but rapid deterioration in moist environment.

The alumina containing materials showed decreasing transformability and fracture resistance but at the same time increasing ageing resistance.

Compared to state-of-the-art coprecipitated 3Y-TZP the materials made from stabilizer coated 2.5Y-TZP powder show superior properties concerning fracture resistance, resistance to subcritical crack growth and low temperature degradation. The materials are thus very attractive for applications operating under high cyclic loads in humid atmosphere. Further investigations will be necessary to scale-up the powder coating process and apply the powders to conventional forming and shaping technologies.

Accomplishments

The authors would like to thank Dr. Hesham El-Maghraby of NRC Cairo, Egypt and Miss Nathalie Rotfuss for assistance in powder preparation and mechanical property measurements.

References

[1] Kelly, P.M., Rose, L.R.F.: The martensitic transformation of ceramics- its role in transformation toughening, *Prog. Mater. Sci.*, 47, (2002), 463-557.
[2] Swain, M.J., Rose, L.R.F.: Strength limitations of transformation toughened alloys, *J. Am. Ceram. Soc.*, 69, 7, (1986), 511-518.
[3] Chevalier, J., Cales, B., Drouin, J.M.: Low temperature ageing of Y-TZP ceramics, *J. Am. Ceram. Soc.*, 82, 8, (1999), 2150-54.
[4] Chevalier, J., Gremillard, L.: Low-Temperature Degradation of Zirconia and Implications for Biomedical Implants, *Annu. Rev. Mater. Res.*, 37, (2007),1–32.
[5] Özkurt, Z., Kazazoglu, E.: Zirconia dental implants: a literature review, *J. Oral Implantol.*, 37, 3, (2011), 367-76.
[6] Wroe, S., Ferrara, T.L., McHenry, C.R., Curnoe, D., Chamoli, U.: The craniomandibular mechanics of being human, Proc. R. Soc. B, 277, (2010), 3579–3586.
[7] Benzaid, R., Chevalier, J., Saadaoui, M., Fantozzi, G., Nawa, M., Diaz, L.D., Torrecillas, R.: Fracture toughness, strength and slow crack growth in a ceria stabilized zirconia–alumina nanocomposite for medical applications, *Biomaterials*, 29, (2008), 3636–41.
[8] Binner, J., Vaidhyanathan, B., Paul, A., Annaporani, K., Raghupathy, B.: Compositional Effects in Nanostructured Yttria Partially Stabilized Zirconia, *Appl. Ceram. Techn.*, 8, 4, (2011), 766-782.
[9] Apel, E., Ritzberger, C., Courtois, N., Reveron, H., Chevalier, J., Schweiger, M., Rothbrust, F., Rheinberger, V.M., Höland, W.: Introduction to a tough, strong and stable Ce-TZP/$MgAl_2O_4$ composite for biomedical applications, *J. Eur. Ceram. Soc.*, 32, 11, (2012), 2697-703.
[10] Singh, R., Gill, C., Lawson, S., Dransfield, G.P.: Sintering, microstructure and mechanical properties of commercial Y-TZPs, *J. Mat. Sci.*, 31, (1996), 6055-62.
[11] Ohnishi, H., Naka, H., Sekino, T., Ikuhara, Y., Niihara, K.: Mechanical properties of 2.0-3.5 mol% Y_2O_3-stabilized zirconia polycrystals fabricated by the solid phase mixing and sintering method, *J. Ceram. Soc. Jap.*,116, (2008), 1270-1277.
[12] Picconi, C., Burger, W., Richter, H.G., Cittadini, A., Maccauro, G., Covacci, V., Bruzzese, N., Ricci, G.A., Marmo, E.: Y-TZP ceramics for artificial joint replacements, *Biomaterials*, 19, (1998), 1489-1494.
[13] Kern, F: Alumina doped 2.5Y-TZP from yttria coated pyrogenic nanopowder, *J. Ceram. Sci. Techn.*, 2, (2011), 89-96.

[14] Ross, I.M., Rainforth, W.M., McComb, D.W., Scott, A.J., Brydson, R.: The role of trace additions to yttria-tetragonal zirconia polycrystals (Y-TZP), *Scripta Materialia*, 45, (2001), 653-60.
[15] Tsukuma, K., Ueda, K.: Strength and fracture toughness of isostatically hotpressed composites of Al_2O_3 and Y_2O_3 partially stabilized ZrO_2, *J. Am. Ceram. Soc*., 68, 1, (1985), C4–5.
[16] Tsubakino, H., Sonoda, K., Nozato, R.: Martensite transformation behaviour during isothermal ageing in partially stabilized zirconia with and without alumina addition, J. *Mater. Sci. Lett*., 12, (1993), 196–8.
[17] Kern, F., Gadow, R.: Alumina toughened zirconia from yttria coated powders, J. *Eur. Ceram. Soc*., 32, 15, (2012), 3911-18.
[18] Yuan, Z.X., Vleugels, J., Van der Biest, O.: Preparation of Y_2O_3-coated ZrO_2 powder by suspension drying, J. Mater. Sci. Lett., 19, (2000), 359–61.
[19] Chantikul, P., Anstis, G.R., Lawn, B.R., Marshall, D.B.: A critical evaluation of indentation techniques for measuring fracture toughness: II, strength method, *J. Am. Ceram. Soc.*, 64, 9, (1981), 539-543.
[20] Dransmann, G.W., Steinbrech, R.W., Pajares, A., Guiberteau, F., Dominguez-Rodriguez, A., Heuer, A.H.: Indentation Studies on Y_2O_3-Stabilized ZrO_2: II, Toughness Determination from Stable Growth of Indentation-Induced Cracks, *J. Am. Ceram. Soc*., 77, 5, (1994), 1194-201.
[21] Toraya, H., Yoshimura, M., Somiya, S.: Calibration curve for quantitative analysis of the monoclinic-tetragonal ZrO_2 system by X-ray diffraction", *J. Am. Ceram. Soc*., 67, 6, (1984), C119–21.
[22] Kosmac, T., Wagner, R., Claussen, N.: X-Ray Determination of Transformation Depths in Ceramics Containing Tetragonal ZrO_2, *J. Am. Ceram. Soc*., 64, 4, (1981), C72–3.
[23] McMeeking, R.M., Evans, A.G.: Mechanics of Transformation--Toughening in Brittle Materials, *J. Am. Ceram. Soc*., 65, 5, (1982), 242-6.
[24] Mendelson, M.I.: Average grain size in polycrystalline ceramics, *J. Am. Ceram. Soc*., 52, 8, (1969), 443-6.
[25] Keuper, M., Eder, K., Berthold, C., Nickel, K.G.: Direct evidence for continuous linear kinetics in the low-temperature degradation of Y-TZP, *Acta Biomaterialia*, 9, 1, (2013), 4826-35.
[26] Swain, M.V.: Grain-size dependence of toughness and transformability of 2 vol.% Y-TZP ceramics, *J. Mat. Sci. Let.*, 5, (1986), 1159-62.

♦

Received 22 August, 2013, accepted 16 September 2013